Calcium signals and calpain-dependent necrosis are essential for release of coxsackievirus B from polarized intestinal epithelial cells

Rebecca A. Bozym[a], Kunal Patel[b], Carl White[c], King-Ho Cheung[d], Jeffrey M. Bergelson[b], Stefanie A. Morosky[a], and Carolyn B. Coyne[a]

[a]Department of Microbiology and Molecular Genetics, University of Pittsburgh, Pittsburgh, PA 15219; [b]Division of Infectious Diseases, Children's Hospital of Philadelphia, Philadelphia, PA 19104; [c]Department of Physiology & Biophysics, Rosalind Franklin University of Medicine and Science, North Chicago, IL 60064; [d]Department of Physiology, University of Hong Kong, Hong Kong

ABSTRACT **Coxsackievirus B (CVB), a member of the enterovirus family, targets the polarized epithelial cells lining the intestinal tract early in infection. Although the polarized epithelium functions as a protective barrier, this barrier is likely exploited by CVB to promote viral entry and subsequent egress. Here we show that, in contrast to nonpolarized cells, CVB-infected polarized intestinal Caco-2 cells undergo nonapoptotic necrotic cell death triggered by inositol 1,4,5-trisphosphate receptor–dependent calcium release. We further show that CVB-induced cellular necrosis depends on the Ca^{2+}-activated protease calpain-2 and that this protease is involved in CVB-induced disruption of the junctional complex and rearrangements of the actin cytoskeleton. Our study illustrates the cell signaling pathways hijacked by CVB, and perhaps other viral pathogens, to promote their replication and spread in polarized cell types.**

Monitoring Editor
Asma Nusrat
Emory University

Received: Feb 2, 2011
Revised: Jun 10, 2011
Accepted: Jun 21, 2011

INTRODUCTION

Enteroviruses, including coxsackievirus B (CVB), are lytic viruses that destroy the host cell membrane for progeny release. Lytic viruses often develop highly efficient strategies to tightly regulate host cell death pathways to avoid killing the host cell prematurely (and terminating viral replication). Studies on the mechanism(s) by which CVB induces host cell death have identified apoptotic signaling, mediated by proapoptotic caspase-3, following CVB infection in HeLa cells (Carthy *et al.*, 1998, 2003; Yuan *et al.*, 2003). CVB encounters the polarized epithelium lining the gastrointestinal tract early in infection, and viral replication in the mucosa is likely followed by epithelial cell lysis and subsequent viremia (Morens and Pallansch, 1995). The precise mechanism(s) by which CVB induces cell death in polarized epithelial cells remains unclear, however.

Viruses can trigger both apoptotic (programmed cell death) and nonapoptotic (necrosis, autophagy) pathways during the course of infection (Agol *et al.*, 1998; Barco *et al.*, 2000; Lopez-Guerrero *et al.*, 2000). Apoptosis is a tightly controlled process of "cell suicide" that is associated with well-characterized morphological and biochemical changes that include fragmentation of DNA, activation of the caspase family of cysteine proteases, and the translocation of phosphatidylserine from the inner to the outer membrane leaflet. Necrosis generally lacks the changes associated with apoptosis, and is instead characterized by irreversible swelling of the cytoplasm and organelles and ultimate lysis of the plasma membrane. Necrosis results in the release of cellular material (often including degradative enzymes) from the cell into the surrounding area that can induce cellular damage to neighboring non-necrotic cells (reviewed in Festjens *et al.*, 2006; Zong and Thompson, 2006).

Many pathogens target intracellular signaling molecules to disrupt normal cell function to facilitate many aspects of their infectious life cycles. The link between alterations in Ca^{2+} homeostasis and cell death pathways has been well established (Trump and Berezesky,

This article was published online ahead of print in MBoC in Press (http://www.molbiolcell.org/cgi/doi/10.1091/mbc.E11-02-0094) on July 7, 2011.

Address correspondence: Carolyn B. Coyne (coynec2@pitt.edu).

Abbreviations used: $[Ca^{2+}]_i$, intracellular Ca^{2+}; CPA, cyclopiazonic acid; CSA, cyclosporine A; CVB, coxsackievirus B; DAPI, 4′,6-diamidino-2-phenylindole; ER, endoplasmic reticulum; IP_3, inositol 1,4,5-trisphosphate; IP_3R, IP_3 receptor; MOI, multiplicity of infection; PBS, phosphate-buffered saline; PFU, particle-forming unit; p.i., postinfection; PI, propidium iodide; PLC, phospholipase C; ROI, region of interest; SERCA, sarco/endoplasmic reticulum Ca^{2+}-ATPase; TER, transepithelial resistance; TJ, tight junction; ZO-1, zonula occludens-1.

Supplemental Material can be found at:
http://www.molbiolcell.org/content/suppl/2011/06/27/mbc.E11-02-0094.DC1.html

1996; Lee *et al.*, 1999; Mattson, 2000; Sattler and Tymianski, 2000; Xu *et al.*, 2001; Orrenius *et al.*, 2003) and has been used by several viruses to promote their infections (reviewed in Zhou *et al.*, 2009). Modulation of intracellular Ca^{2+} ($[Ca^{2+}]_i$) signaling has been implicated in both pro- and antiapoptotic pathways and is a key component in the activation of necrotic cell death and autophagy (Hoyer-Hansen *et al.*, 2007; Hoyer-Hansen and Jaattela, 2007; Cardenas *et al.*, 2010). Thus levels of Ca^{2+} are tightly regulated by the cell as a means to control both the induction and inhibition of numerous types of cell death. The release of Ca^{2+} by inositol 1,4,5-trisphosphate (IP_3) receptor (IP_3R)-dependent mechanisms can induce apoptosis through mitochondrial transfer of Ca^{2+} (and the subsequent release of proapoptotic factors into the cytoplasm) or through the activation of Ca^{2+}-sensitive proapoptotic enzymes within the cytoplasm. In some cases, the expression of IP_3R is involved for the induction of apoptosis: Reducing IP_3R expression in both chicken lymphoma (Sugawara *et al.*, 1997) and human T-cells (Jayaraman and Marks, 1997) renders them resistant to apoptosis.

The link between Ca^{2+} release and the activation of necrotic cell death is also striking. Like apoptosis, necrotic cell death is often initiated by dramatic alterations in mitochondrial Ca^{2+} homeostasis resulting from endoplasmic reticulum (ER)-localized Ca^{2+} release and the concomitant activation of the Ca^{2+}-activated calpain family of cysteine proteases. Members of the calpain family can be categorized into two subfamilies: μ-calpains (or calpain-1, are activated by micromolar concentrations of Ca^{2+}) and m-calpains (or calpain-2, are activated by millimolar concentrations of Ca^{2+}) (reviewed in Liu *et al.*, 2004). After being activated by autocatalytic hydrolysis, calpains translocate from the cytosol to intracellular membranes, where they are primed to cleave a number of diverse substrates. Calpain substrates can include cytoskeletal proteins, adhesion molecules, membrane proteins, kinases, phosphatases, ion transporters, and phospholipases (Rami, 2003). The mechanisms by which the cell "decides" to undergo either apoptosis or necrosis may depend on the nature of the insult and/or on the signaling pathways involved in modulating the various cell death pathways.

Here we show that, in contrast to nonpolarized cells, polarized intestinal Caco-2 cells do not undergo apoptosis in response to CVB infection and instead undergo a caspase-independent form of necrotic cell death. Whereas release of progeny virus from nonpolarized cells occurred by a caspase-dependent process, CVB release from Caco-2 cells occurred in a caspase-independent manner and was instead mediated specifically through calpain-2. We further show that CVB infection of Caco-2 cells results in an early (~2 h postinfection [p.i.]) increase in $[Ca^{2+}]_i$ that is followed by $[Ca^{2+}]_i$ depletion occurring between 2 and 3 h p.i. CVB-induced Ca^{2+} release required the activity of phospholipase C (PLC) and the expression of IP_3Rs, and inhibiting the activity or expression of these factors prevented CVB progeny release. Taken together, these findings indicate that the host cell factors manipulated by CVB to induce cell death and subsequent progeny release may differ among cell types and that CVB exploits PLC-dependent Ca^{2+} release to promote its escape from polarized intestinal cells.

RESULTS

CVB-induced cell death in polarized intestinal epithelial cells is caspase-independent

Proapoptotic signals mediated by activated caspase-3 have been associated with CVB-induced cell death in nonpolarized cell types (Carthy *et al.*, 1998; Yuan *et al.*, 2003). Consistent with this, we found that CVB infection of HeLa cells led to the activation of caspase-3 (as determined by the appearance of cleaved caspase-3 by immunoblotting) within 3–4 h p.i. (Figure 1A). In contrast, we found no enhancement in cleaved caspase-3 in CVB-infected polarized intestinal epithelial Caco-2 cells (Figure 1A). Both CVB–infected HeLa and Caco-2 cells died within 7–10 h after infection, showing gross morphological changes and loss of membrane integrity as detected by uptake of propidium iodide (PI) (Figure 1B). Whereas CVB-infected HeLa cells displayed changes consistent with apoptosis, including externalization of phosphatidylserine (detectible by Annexin V binding), CVB-infected Caco-2 cells did not exhibit any detectable Annexin V binding (Figure 1B). This effect was not specific to Caco-2 cells as we observed the lack of Annexin V binding to other CVB-infected polarized epithelial cells (HCT-116 and HT-29; Supplemental Figure 1). Moreover, we also found that CVB-infected Caco-2 cells did not exhibit apoptosis-associated DNA fragmentation as assessed by terminal deoxynucleotidyl transferase dUTP nick end labeling (TUNEL) assay, whereas infected HeLa cells did (Supplemental Figure 2A). We confirmed that Caco-2 cells were capable of undergoing apoptosis by incubating cells with the apoptosis-inducing agent staurosporine, which led to enhanced Annexin V binding (Supplemental Figure 2B).

We also found that whereas the caspase inhibitor Z-VAD-FMK prevented Annexin V binding and PI uptake in CVB-infected HeLa cells (Figure 1C), it had no effect on PI uptake in CVB-infected Caco-2 cells (Figure 1D). Furthermore, we found that whereas Z-VAD-FMK inhibited viral egress from CVB-infected HeLa cells, it had no effect on CVB release from infected Caco-2 cells (Figure 1, E and F). Taken together, these data indicate that, in contrast to nonpolarized cells, the loss of membrane integrity in CVB-infected Caco-2 cells occurs via a caspase-independent mechanism.

Calpains are involved in CVB-induced necrosis in Caco-2 cells

Necrotic cell death fails to display many of the classical features (such as phosphatidylserine externalization) associated with apoptotic cell death, but is still associated with the loss of plasma membrane integrity. The activation of Ca^{2+}-sensitive calpain proteases often contributes to the onset of necrosis (Wang, 2000; Liu *et al.*, 2004). Because CVB appeared to kill Caco-2 cells by a nonapoptotic mechanism, we tested whether calpain-dependent necrosis might be important. We found that treatment of Caco-2 cells with the calpain inhibitor Z-Val-Phe-CHO inhibited the increase in membrane permeability associated with cell death induced by CVB infection (as assessed by PI uptake) (Figure 2A) but had no effect on CVB replication (Figure 2, A and B). Furthermore, we found that Z-Val-Phe-CHO prevented the release of CVB particles from infected Caco-2 cells but had minimal effect on virus titers (Figure 2C).

To identify the time period during which calpain activity was required to induce CVB-mediated increases in membrane permeability, we performed a time-of-addition experiment in which Z-Val-Phe-CHO was added at various times p.i. We found that Z-Val-Phe-CHO exerted its most potent inhibitory effects when added to CVB-infected cultures before 2–3 h p.i. (Figure 2D). Whereas Z-Val-Phe-CHO partially inhibited CVB-induced PI uptake at 4 h p.i., it had no effect when added at >5 h p.i. (Figure 2D). Consistent with this result, we found a slight elevation in overall calpain activity in cells infected with CVB that peaked at 2–3 h p.i., but returned to control levels by 4 h p.i. (Supplemental Figure 4). Taken together, these data indicate that calpains are likely activated early in CVB infection (~2–3 h p.i.).

Calpain-2 is specifically involved in CVB-induced necrosis

We found that calpains were required for alterations in membrane permeability required for CVB egress in Caco-2 cells (Figure 2, A

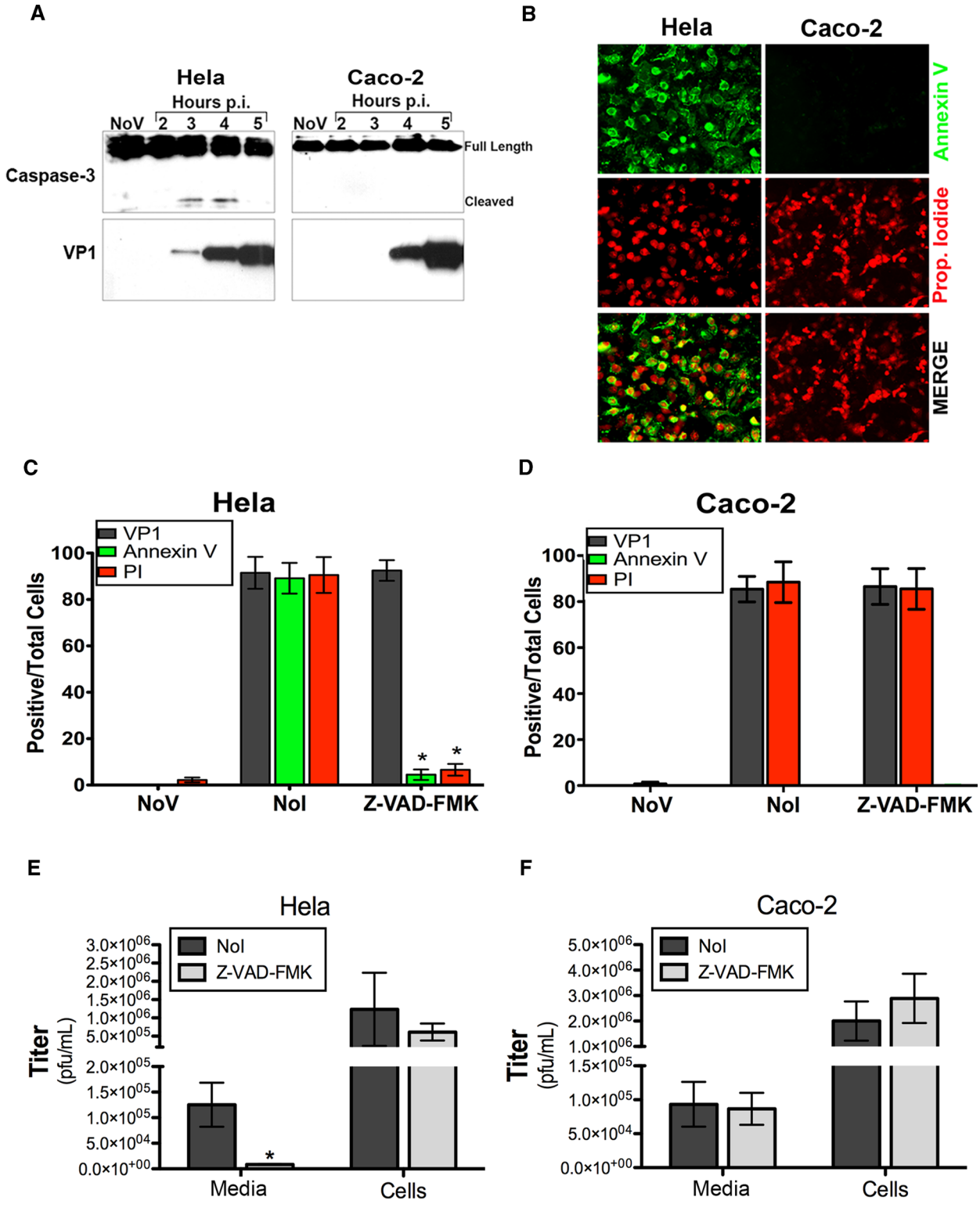

FIGURE 1: Caco-2 cells infected with CVB do not undergo apoptosis. (A) Western blot analysis of caspase-3 (top) and VP1 (bottom) in HeLa and Caco-2 cells at the indicated times following CVB infection. (B) Annexin V (green) binding and PI (red) uptake in HeLa (left) or Caco-2 (right) cells infected with CVB for 8 h. (C and D) Quantification of immunofluorescence images of Annexin V binding, PI uptake, and infection (as determined by VP1 immunofluorescence) in CVB-infected HeLa (C) or Caco-2 (D) cells incubated with no inhibitor (NoI), with the caspase-3 inhibitor Z-VAD-FMK, or in uninfected (NoV) controls. Data are presented as the percentage of positive cells divided by the total number of cells. (E and F) Virus titers (shown as PFU/ml) determined by plaque assays from the medium vs. lysed cells of HeLa (E) or Caco-2 (F) cells infected with CVB for 12 h in the absence (no inhibitor, NoI) or presence of Z-VAD-FMK. In (C–F), data are presented as mean ± SD from experiments performed in triplicate a minimum of three times, *$p < 0.001$.

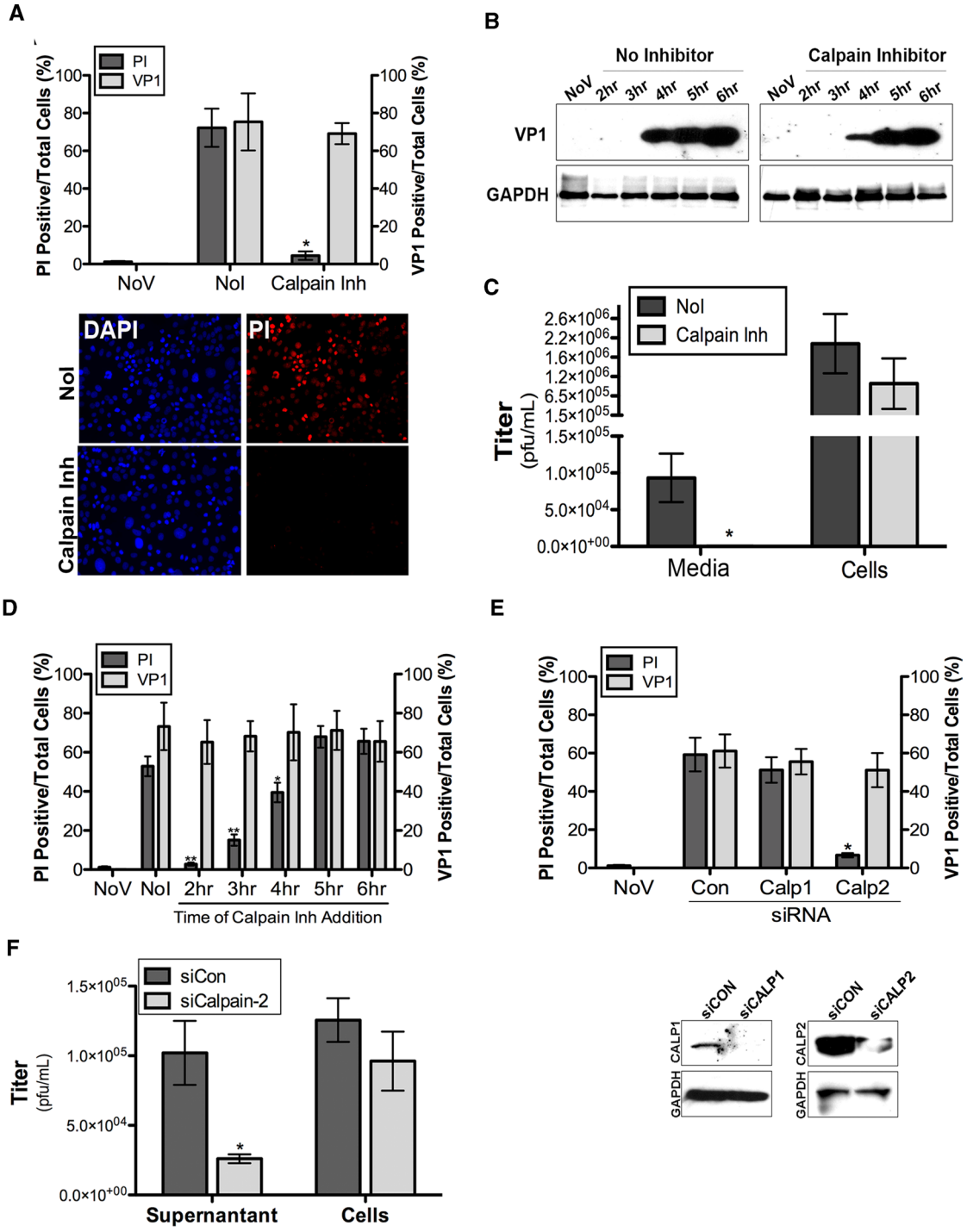

FIGURE 2: Calpains mediate CVB-induced necrosis in Caco-2 cells. (A) PI uptake and VP1 staining in Caco-2 cells infected with CVB for 8 h in the absence of inhibitor (NoI), in the presence of the calpain inhibitor Z-Val-Phe-CHO, or in uninfected (NoV) controls. Representative images of DAPI (blue) and PI (red) are shown. (B) Western blot analysis for VP1 in Caco-2 cells infected with CVB for the indicated time in the absence of inhibitor (left) or in the presence of Z-Val-Phe-CHO (right). GAPDH is shown at bottom as a loading control. (C) Virus titers (shown as PFU/ml) determined by plaque assays from the medium vs. lysed cells of Caco-2 cells infected with CVB for 12 h in the absence (no inhibitor, NoI) or presence of Z-Val-Phe-CHO. (D) Percent PI uptake and VP1 staining in Caco-2 cells infected with CVB in the absence (NoI) or presence of Z-Val-Phe-CHO added to cells at the indicated times p.i. or in uninfected (NoV) controls. Shown are the percentages of PI- or VP1-positive cells divided by the total number of cells. (E) Percent PI uptake and VP1 staining in Caco-2 cells transfected with control (Con) or calpain-1 or -2 siRNAs (by Amaxa nucleofection) and infected with CVB (for 8 h) 48 h posttransfection. Shown are the percentages of PI- or VP1-positive cells. Bottom, immunoblot analysis for calpain-1 (left) or -2 (right) in siRNA-transfected cells. GAPDH is included as a loading control. (F) Virus titers (shown as PFU/ml) determined by plaque assays from the medium vs. lysed cells of Caco-2 cells transfected with control siRNA or calpain-2 siRNA (by Amaxa nucleofection) and infected with CVB for 12 h. In (C–F), data are presented as mean ± SD from experiments performed in triplicate a minimum of three times, *$p < 0.05$ and **$p < 0.001$.

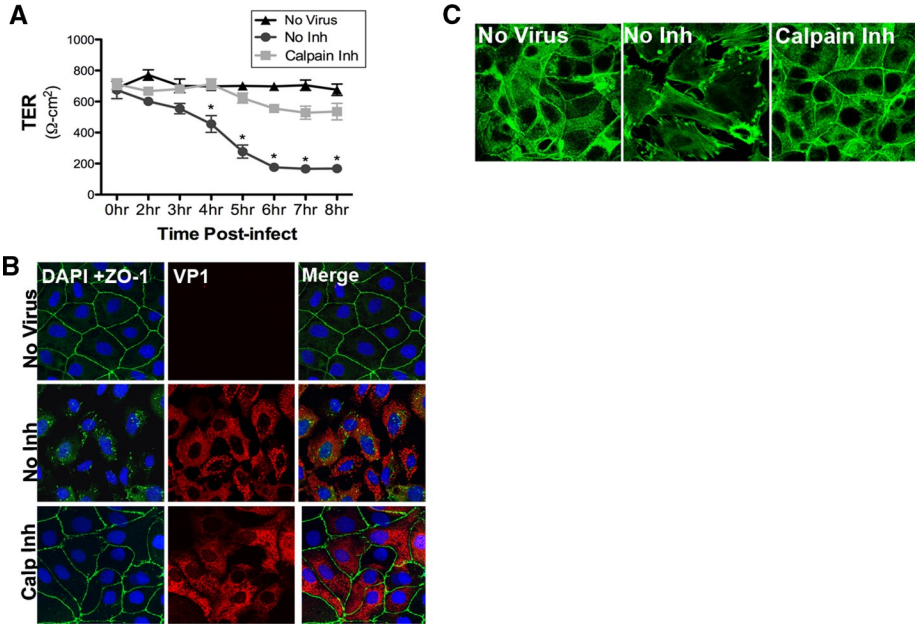

FIGURE 3: Loss of junctional integrity in CVB-infected Caco-2 cells. (A) TER measurements in Caco-2 cells infected with CVB in the absence (No Inh) or presence of Z-Val-Phe-CHO (Calpain Inh) for the indicated times or in uninfected (no virus) controls. (B) Confocal micrographs of Caco-2 cells infected with CVB for 8 h in the absence (No Inh) or presence of Z-Val-Phe-CHO and stained for DAPI (blue), ZO-1 (green), and VP1 (red) compared with uninfected (no virus) controls. (C) Immunofluorescence microscopy staining for actin in Caco-2 cells infected with CVB for 8 h in the absence (No Inh) or presence of Z-Val-Phe-CHO (Calpain Inh) or in uninfected controls.

and C). Members of the calpain family can be categorized into two subfamilies: μ-calpains (or calpain-1) and m-calpains (or calpain-2) based on their sensitivity to Ca^{2+} (reviewed in Liu *et al.*, 2004). To determine which member of the calpain family was involved in CVB-induced necrosis, we down-regulated either calpain-1 or -2 expression in Caco-2 cells by RNAi and determined the effects of this on CVB-induced membrane permeability. We found that whereas down-regulation of calpain-1 had no effect on PI uptake in CVB-infected cells, calpain-2 small interfering RNA (siRNA) significantly reduced PI uptake while having no effect on CVB replication (Figure 2E). Furthermore, we found that down-regulation of calpain-2 expression by siRNA transfection significantly inhibited CVB release from infected cells (Figure 2F). These data point to a role for calpains in CVB-mediated escape from infected Caco-2 cells.

Calpains mediate tight junction and actin cytoskeletal reorganization in CVB-infected Caco-2 cells

Polarized epithelial cells are characterized by the presence of distinct apical and basolateral domains separated by junctional complexes composed in part by the apical tight junction (TJ) complex. We found that CVB infection of Caco-2 cells led to a loss of TJ integrity as assessed by decreased transepithelial resistances (TERs) within 4 h p.i. (Figure 3A) and relocalization of the TJ-associated component zonula occludens-1 (ZO-1) (Figure 3B). Activated calpains target a number of molecules associated with maintaining polarized cell architecture, such as components of apical TJ complexes and components associated with actin cytoskeletal stability (Rios-Doria *et al.*, 2003; Franco *et al.*, 2004; Lebart and Benyamin, 2006). We found that incubation of cells with Z-Val-Phe-CHO inhibited CVB-induced decreases in TER and ZO-1 relocalization (Figure 3, A and B), indicating that this process requires calpain activity. We also found pronounced alterations in the actin cytoskeleton in CVB-infected cells that were characterized by loss of junction-associated actin and increased stress fiber formation (Figure 3C). CVB-induced alterations in actin cytoskeleton architecture were also inhibited by Z-Val-Phe-CHO (Figure 3C), indicating that calpains also mediate the modulation of actin cytoskeletal architecture.

Calpains target components of junctional complexes in CVB-infected Caco-2 cells

Calpains regulate a variety of actin-dependent cellular processes and have been implicated in the maintenance of cell adhesion and in the control of cellular motility. The direct proteolysis of actin- and junction-associated cellular components is likely central to calpain-dependent regulation of these processes. Calpains have been shown to cleave (in vitro and/or in vivo) the cytoskeletal proteins talin, vinculin, and paxillin and the junction-associated proteins occludin, E-cadherin, and β-catenin (Rios-Doria *et al.*, 2003; Franco *et al.*, 2004; Lebart and Benyamin, 2006; Chun and Prince, 2009). Because we observed calpain-dependent alterations in TER and rearrangements of the actin cytoskeleton, we investigated the expression pattern of known calpain substrates in CVB-infected Caco-2 cells. We found that many calpain substrates were unaffected by CVB infection including Ezrin, paxillin, talin, vinculin, and ZO-1 (Figure 4A). We observed the appearance, however, of a distinct cleavage fragment of the TJ-associated transmembrane protein occludin in CVB-infected cultures that could be blocked by treatment of cells with Z-Val-Phe-CHO (Figure 4A). In addition, we found that CVB infection elicited significant decreases in the expression of both β-catenin and E-cadherin that were restored when cells were infected in the presence of Z-Val-Phe-CHO (Figure 4A). We also found that both occludin cleavage and E-cadherin down-regulation occurred in a time-dependent manner in CVB-infected cells and that both events were evident by 3–4 h p.i. but were most prominent at 6 h p.i. (Figure 4B). In contrast, the expression of ZO-1 did not exhibit any significant decreases, nor did we detect any cleavage fragments in response to CVB infection (Figure 4, A and B). Taken together, these data indicate that CVB infection elicits the cleavage and/or down-regulation of several junction-associated membrane components and that calpains likely play a central role in these processes.

We also observed extensive rearrangements of occludin and E-cadherin (unpublished data) localization including a loss of junctional association and corresponding appearance of intracellular occludin-containing vesicles in CVB-infected cells (Figure 4C). The redistribution of occludin was inhibited in CVB-infected cells treated with Z-Val-Phe-CHO, indicating that calpains likely mediate some event in the cleavage and subsequent relocalization of occludin.

As we observed alterations in two components of the junctional complex in CVB-infected Caco-2 cells, we next examined the subcellular localization of calpains in infected cultures. Calpains localize predominantly to the cytosol but, upon exposure to Ca^{2+}, translocate to a variety of intracellular membranes where they undergo autolysis and subsequent activation (Michetti *et al.*, 1996; Glading

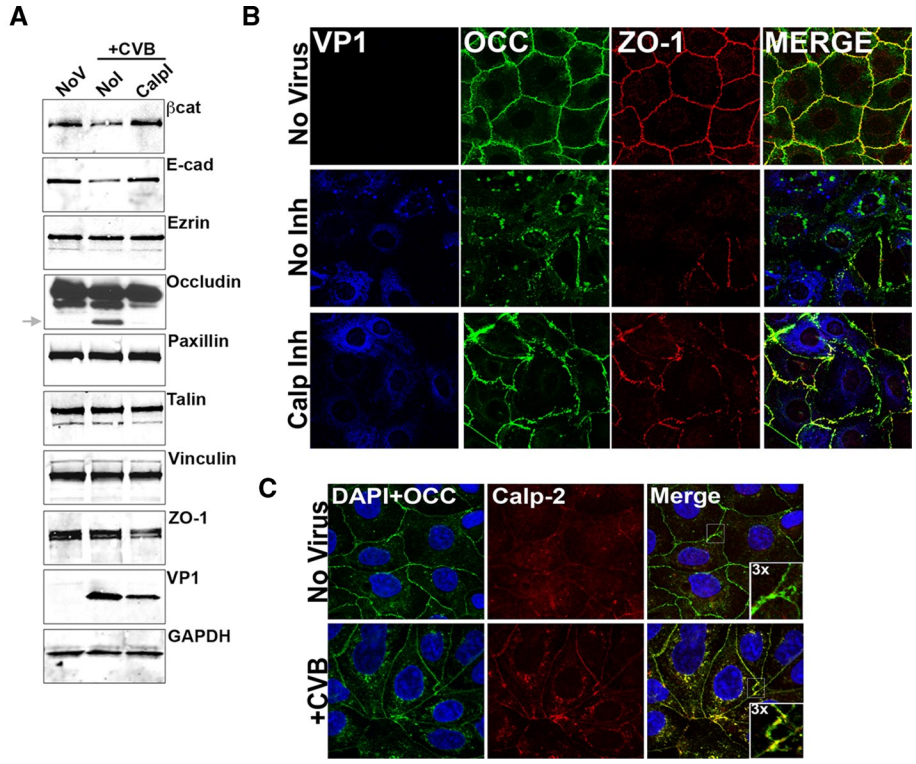

FIGURE 4: Several junction-associated components are modulated by calpains during CVB infection. (A) Western blot analysis for the indicated proteins from lysates of Caco-2 cells infected with CVB for 12 h in the absence (NoI) or presence of Z-Val-Phe-CHO (CalpI) or in uninfected controls (NoV). GAPDH is shown as a loading control, and VP1 production is shown as a control for infection levels. Arrow (gray) denotes a cleaved occludin fragment. (B) Western blot analysis for occludin, E-cadherin, and ZO-1 from lysates of Caco-2 cells infected with CVB for the indicated times. VP1 production is shown as a control for infection levels. Arrow (gray) denotes a cleaved occludin fragment. (C) Confocal micrographs of Caco-2 cells stained for VP1 (blue), occludin (green), and ZO-1 (red) in the absence of virus or in cells infected with CVB for 8 h in the absence or presence of calpain inhibitor Z-Val-Phe-CHO. (D) Confocal micrographs of Caco-2 cells stained for DAPI (blue), occludin (green), or calpain-2 (red) in the absence or presence of CVB 3 h p.i.

et al., 2001; Leloup *et al.*, 2010). Relocalization of activated calpains thus serves to facilitate substrate cleavage. We found that CVB infection of Caco-2 cells induced the cleavage and/or downregulation of β-catenin, E-cadherin, and occludin, all components known to localize to cell–cell junctions. Interestingly, we observed the relocalization of calpain-2 to sites of cell–cell contact and to intracellular vesicles where it colocalized with occludin within 4 h following CVB infection (Figure 4D). We also found that Z-Val-Phe-CHO lost its inhibitory effect when added 2–3 h p.i. (Figure 2D). Taken together, these data indicate that calpain-2 is likely activated before to 4 h p.i. and is then translocated to cellular junctions where it cleaves several components of the junctional complex, thus disrupting junctional architecture, cell–cell contacts, and cell polarity.

Inhibitors of ER-derived Ca^{2+} release block CVB-induced necrosis

Because alterations in $[Ca^{2+}]_i$ homeostasis are essential for calpain activation, we next determined the effect of a panel of pharmacological inhibitors known to modulate intracellular calcium signaling on CVB-induced necrosis and identified a number of inhibitors that prevented cell death but had no effect on CVB infection (Figure 5A). These included Bapta-AM, a $[Ca^{2+}]_i$ chelator; caffeine, which causes release of Ca^{2+} stores by activating ryanodine receptors; cyclopiazonic acid (CPA), an inhibitor of sarco/endoplasmic reticulum Ca^{2+}-ATPase (SERCA)-mediated Ca^{2+} uptake; and thapsigargin, a specific inhibitor of SERCAs that results in depletion of ER-derived Ca^{2+} stores. In contrast, cyclosporine A (CSA), an inhibitor of the mitochondrial permeability transition pore, had no effect on either necrosis or virus replication (Figure 5A).

These results point to a role for ER-derived release of Ca^{2+} in CVB-induced necrosis and suggest that the release of mitochondrial Ca^{2+} stores did not play a significant role in this process. Consistent with this result, we found that 2-APB, an inhibitor of IP_3Rs, and U73122, an inhibitor of PLC, also prevented CVB-induced necrosis (Figure 5B).

Release of ER Ca^{2+} stores was also required for alterations in actin cytoskeletal and TJ integrity, as we found that thapsigargin inhibited CVB-induced reorganization of ZO-1 (Supplemental Figure 3) and occludin (Figure 5C). Furthermore, thapsigargin, U73122, and 2-APB all inhibited CVB release from infected Caco-2 cells (Figure 5D). These data point to a role for PLC-dependent activation and subsequent release of Ca^{2+} via ER-localized IP_3R channels in alterations in membrane integrity required for CVB release from Caco-2 cells.

CVB infection depletes ER-derived Ca^{2+} stores early in infection

To better define the time period during which Ca^{2+} signaling was required to induce necrosis, we performed a time-of-addition experiment in which thapsigargin, U73122, and 2-APB were added at various times p.i. We found that all three drugs maintained their inhibitory effects when added to cells 2–3 h p.i., but lost their effectiveness when added at 4 h p.i. (Figure 5E). Interestingly, these kinetics were similar to the pattern we had observed with a calpain inhibitor (Figure 2D). Taken together, these data suggest that alterations in cellular Ca^{2+} signaling likely occur early in CVB infection, by 3–4 h p.i.

To more precisely measure the effect of CVB infection on ER Ca^{2+} stores, we monitored the level of Ca^{2+} release in response to the addition of thapsigargin at various times p.i. Whereas uninfected control cells exhibited pronounced release of Ca^{2+} stores upon exposure to thapsigargin (Figure 6, A and B), cells infected with CVB for 3 h displayed a marked decrease in Ca^{2+} release in response to thapsigargin (Figure 6, A and B). At 2 h p.i., we also observed a decrease in Ca^{2+} release compared with uninfected controls (Supplemental Figure 5). After 3 h p.i., we were unable to measure Ca^{2+} levels in CVB-infected cells because necrosis-induced increases in membrane permeability made it impossible to load cells with calcium-sensitive dye.

Next we monitored real-time Ca^{2+} signaling in cells infected with CVB. As we had observed a reduction in thapsigargin-sensitive Ca^{2+} release in CVB-infected cells at 3 h p.i., we monitored real-time

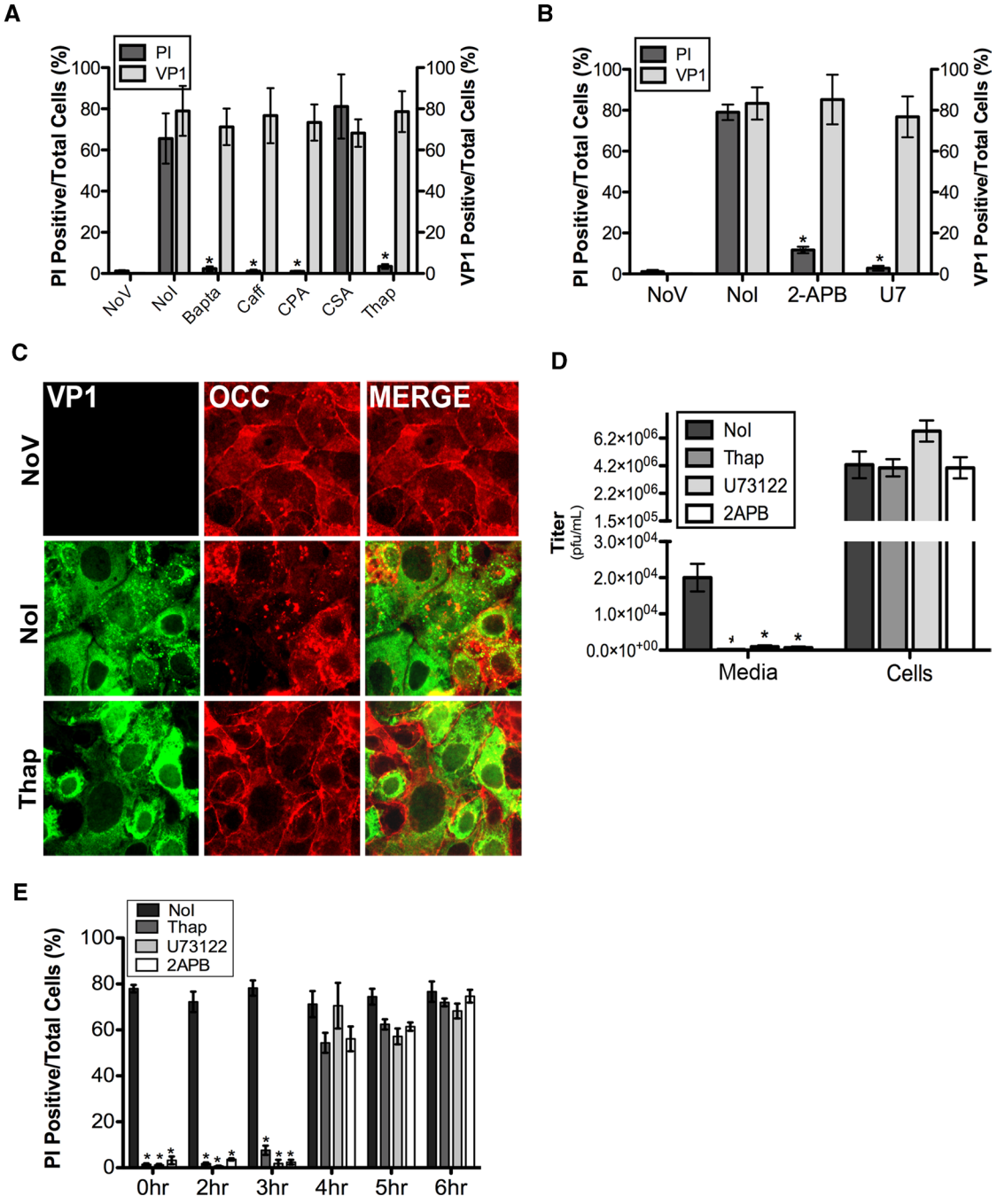

FIGURE 5: Pharmacological inhibitors of calcium homeostasis or signaling prevent CVB-induced necrosis in Caco-2 cells. (A) PI uptake and VP1 staining (shown as percent positive staining divided by the total number of cells) in Caco-2 cells infected with CVB for 8 h in the absence of inhibitor (NoI) or in the presence of the indicated inhibitors [Bapta-AM, caffeine (Caff), CPA, CSA, or thapsigargin (Thap)] or in uninfected (NoV) controls. (B) PI uptake and VP1 staining (shown as percent positive staining divided by the total number of cells) in Caco-2 cells infected with CVB for 8 h in the absence of inhibitor (NoI) or in the presence of the indicated inhibitors [2-APB or U73122 (U7)] or in uninfected (NoV) controls. (C) Immunofluorescence microscopy for VP1 (green) and occludin (red) in Caco-2 cells infected with CVB for 8 h in the absence (NoI) or presence of thapsigargin (Thap), or in uninfected (NoV) controls. (D) Virus titers (shown as PFU/ml) determined by plaque assays from the medium vs. lysed cells of Caco-2 cells infected with CVB for 12 h in the absence [no inhibitor, NoI] or presence of thapsigargin (thap), U73122, or 2-APB. (E) Percent PI uptake in Caco-2 cells infected with CVB for 8 h in the absence (NoI) or presence of thapsigargin (thap), U73122, or 2-APB added to cells at the indicated times p.i., or in uninfected (NoV) controls. Shown are the percentages of PI-positive cells divided by the total number of cells. Data in (A, B, D, and E) are presented as mean ± SD from experiments performed in triplicate a minimum of three times, *$p < 0.001$.

changes in $[Ca^{2+}]_i$ over the course of infection over 1 h (spanning from 2 to 3 h p.i.). We found that whereas Ca^{2+} levels remained stable in uninfected cells over the course of 1 h, there was a pronounced decrease in Ca^{2+} in CVB-infected cells between 2 and 3 h p.i. (Figure 6, C and D). These data indicate that alterations in ER Ca^{2+} stores occur early in CVB infection (between 2 and 3 h p.i).

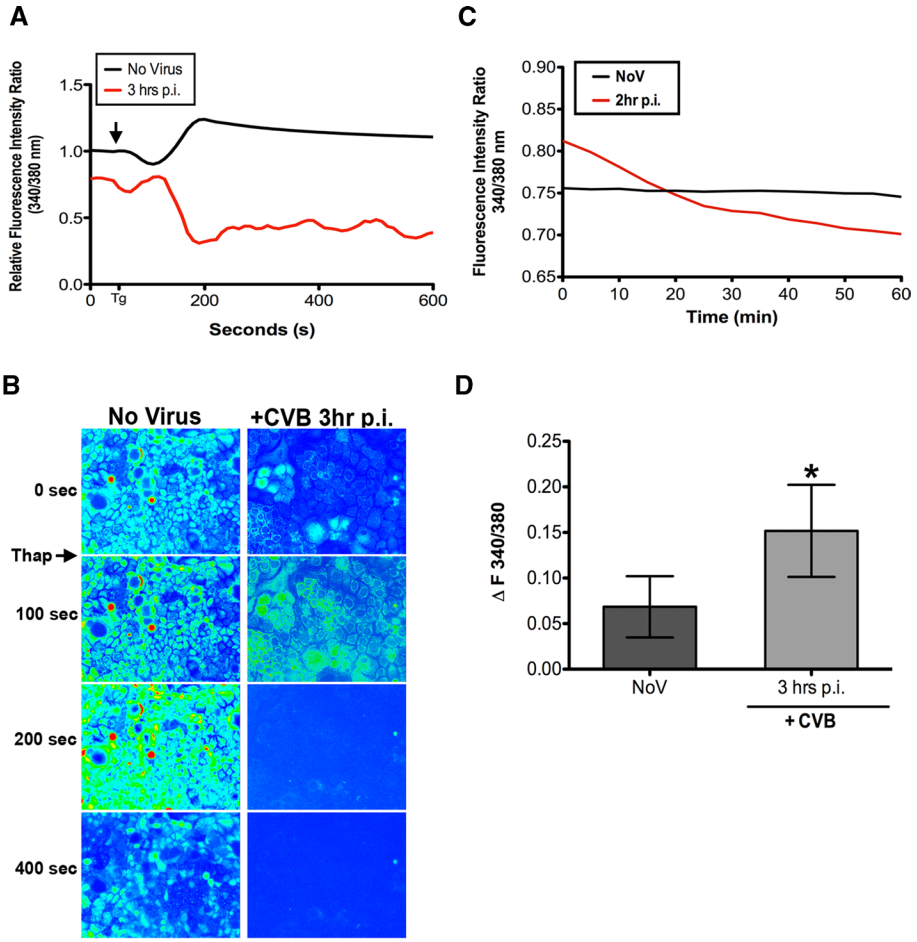

FIGURE 6: $[Ca^{2+}]_i$ stores are depleted between 2 and 3 h following CVB infection of Caco-2 cells. (A) Fluorescence intensity ratio of Fura-2 in response to thapsigargin (black arrow) in Caco-2 cells infected with CVB for 3 h or in uninfected (No Virus) controls. Shown are representative traces per condition. (B) Representative images of Fura-2 AM–loaded Caco-2 cells from (A). Time of thapsigargin addition is represented by a black arrow. Images are pseudocolored for visual assessment with dark blue (low Ca^{2+}) and red (high Ca^{2+}). (C) Fluorescence intensity ratio over the course of 1 h in Caco-2 cells infected with CVB for 2 h (2–3 h p.i.) or in uninfected controls. (D) Change in intensity ratio from traces shown in (C). Data in (D) are presented as mean ± SD from experiments performed in triplicate a minimum of three times, *$p < 0.0001$.

CVB-mediated depletion of ER-derived Ca^{2+} requires PLC and IP_3Rs

To determine whether CVB-induced depletion of ER Ca^{2+} stores involved IP_3 production and/or IP_3Rs, we tested the effects of pharmacological inhibitors of PLC (U73122) and IP_3R function (2-APB). Cells were treated with inhibitors and infected with CVB for 3 h, then thapsigargin was added and ER-derived Ca^{2+} release was measured. In the absence of inhibitors, CVB-infected cells exhibited significantly smaller changes in $[Ca^{2+}]_i$ in response to thapsigargin than did uninfected controls (Figure 7, A and B). In contrast, after treatment with U73122 or 2-APB, the response to thapsigargin was the same in both CVB-infected and uninfected control cells (Figure 7, A and B).

To further define the role of IP_3Rs in CVB-induced alterations in $[Ca^{2+}]_i$, we transfected cells with siRNAs targeted against IP_3R-1 and -3, which are expressed in Caco-2 cells (there were no detectable levels of IP_3R-2 found in these cells; unpublished data) and measured the effect of combined IP_3R-1 and -3 depletion on thapsigargin-sensitive Ca^{2+} stores in CVB-infected cells. Similar to our findings with 2-APB, we found that transfection of cells with IP_3R-1 and -3 siRNAs prevented the depletion of thapsigargin-sensitive ER Ca^{2+} stores in CVB-infected cells (Figure 7, C and D). Moreover, we found that depletion of IP_3R-1 and -3 expression by RNAi prevented the release of CVB progeny from infected Caco-2 cells but had no effect on virus titers (Figure 7, E and F).

DISCUSSION

Although pathogens likely hijack multiple host cell signaling cascades during infection, the precise cascade of signals that culminates in the release of enteroviruses from host polarized cells have remained unclear. Here we show that, in polarized intestinal epithelial cells, CVB infection leads to the release of ER-derived Ca^{2+} to induce a cascade of events resulting in the destruction of the host cell membrane as a means to promote progeny release. CVB specifically exploits IP_3R-dependent Ca^{2+} release to induce nonapoptotic necrotic cell death and involves the activation of the Ca^{2+}-activated protease calpain-2. Activated calpain-2 is involved in the cleavage and/or down-regulation of β-catenin, E-cadherin, and occludin, all components of epithelial TJs and cell–cell contacts, which likely contributes to CVB-induced loss of cell polarity and adhesion. These findings point to a novel role for $[Ca^{2+}]_i$ signaling in the release of CVB from polarized epithelia and suggest that the signals necessary for multiple steps in the virus life cycle may differ between polarized and nonpolarized cells types.

Alterations in cellular Ca^{2+} homeostasis play a fundamental role in the response of many tissue types to injury or assault. We found that CVB infection induced the depletion of thapsigargin-sensitive Ca^{2+} stores by 3 h p.i. and that several pharmacological inhibitors targeting $[Ca^{2+}]_i$ signaling lost their inhibitory effects between 2 and 3 h p.i. Other investigators have reported that the CVB protein 2B perturbs Ca^{2+} homeostasis in HeLa cells by directly modifying ER membrane permeability to promote virus release (van Kuppeveld *et al.*, 1997). The effects we observe on Ca^{2+} homeostasis occurred by 2–3 h p.i., a time before the detection of newly synthesized viral RNA and protein (which generally occurs at ~4 h p.i. in Caco-2 cells; Figure 1A and unpublished data), which would indicate that low levels of 2B are likely present at these times. Moreover, our observations suggest that the depletion of ER Ca^{2+} stores induced by CVB infection of Caco-2 cells involves the initiation of PLC-dependent signaling cascades, as we observed that pharmacological inhibitors of PLC, an IP_3R antagonist (2-APB), and RNAi-mediated down-regulation of IP_3R-1 and -3 inhibited CVB-induced Ca^{2+} release. Although CVB 2B may contribute to further Ca^{2+} alterations induced at later stages of CVB replication, our data indicate that PLC-dependent activation of IP_3Rs contributes primarily to the release of Ca^{2+} required to initiate necrosis and facilitate calpain activation in Caco-2 cells.

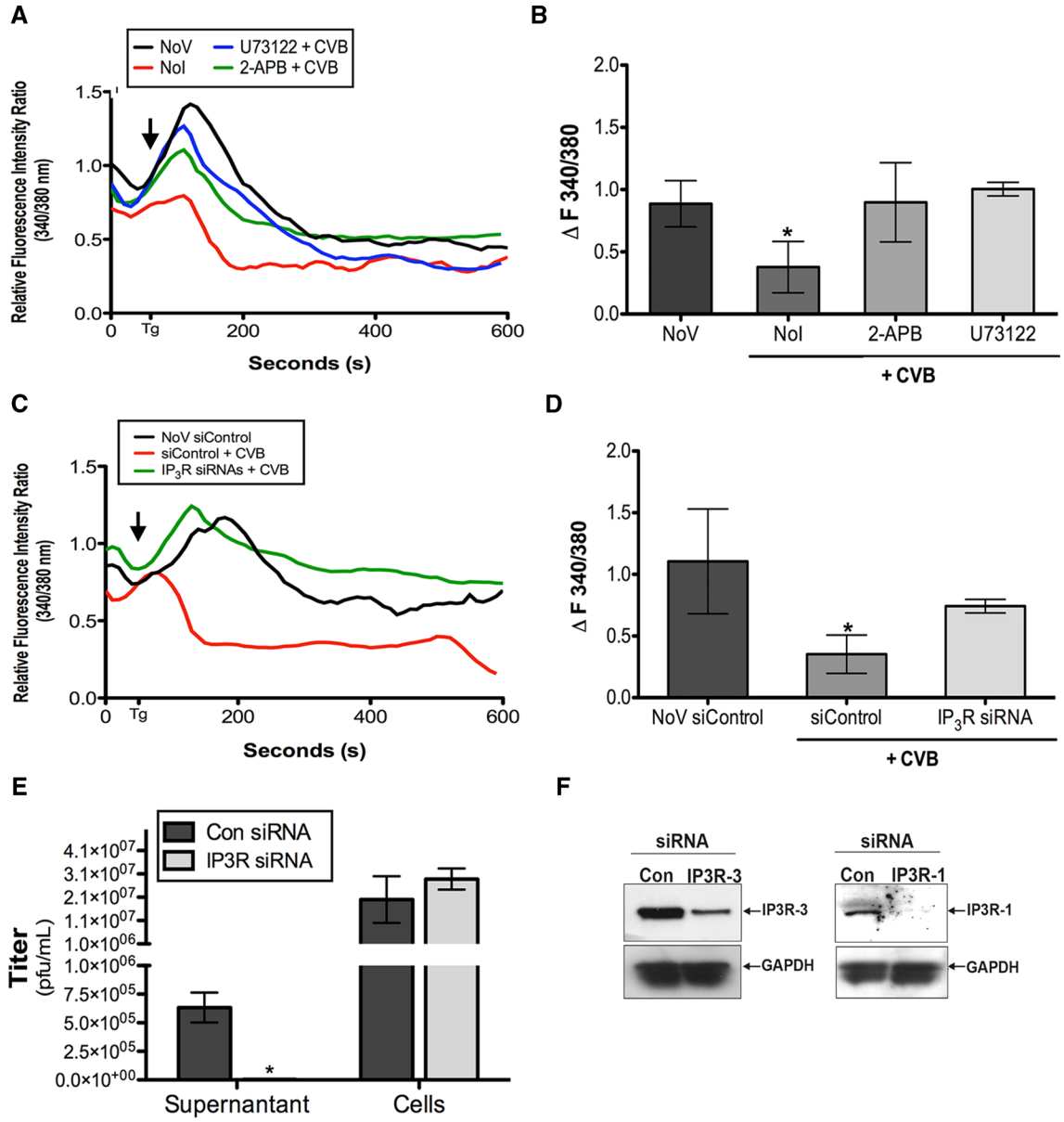

FIGURE 7: PLC activity and IP_3R expression are required for CVB-induced alterations in Ca^{2+}. (A) Fluorescence intensity ratio over time in response to thapsigargin (black arrow) in Caco-2 cells infected with CVB for 3 h p.i. in the absence (NoI) or presence of 2-APB or U73122 or in uninfected (NoV) controls. (B) Overall change in fluorescence intensity ratio from traces shown in (A). (C) Fluorescence intensity ratio over time in response to thapsigargin (black arrow) in Caco-2 cells cotransfected with control or IP_3R-1 and -3 siRNAs (using Hiperfect) and infected (48 h posttransfection) with CVB for 3 h. (D) Overall change in fluorescence intensity ratio from traces shown in (C). (E) Virus titers (shown as PFU/ml) determined by plaque assays from the medium vs. lysed cells of Caco-2 cells transfected with control (CON) or IP_3R-1 and -3 siRNAs (by Amaxa nucleofection) and infected with CVB for 12 h. Data in (B), (D), and (E) are presented as mean ± SD from experiments performed in triplicate a minimum of three times, *$p < 0.001$. (F) Western blot analysis for IP_3R-1 and -3 expression in Caco-2 cells transfected with control siRNA or siRNAs against IP_3R-1 or -3. GAPDH is shown as a loading control.

Calpains are ubiquitously expressed, Ca^{2+}-dependent proteases that are categorized based on the Ca^{2+} concentration required for their activation. Our results indicate that calpain-2 plays a key role in promoting CVB-induced host cell necrosis, as inhibition of calpain activity or RNAi-mediated silencing of calpain-2 prevented CVB egress from polarized epithelial cells. Interestingly, apicomplexan parasites, including *Plasmodium falciparum* and *Toxoplasma gondii*, have also been shown to use calpains to facilitate their egress from infected cells, although the mechanism by which they activate these proteases remains unclear (Chandramohanadas *et al.*, 2009). Our data indicate that calpain activity is required to induce a loss of polarity and junctional integrity that accompanies CVB infection of Caco-2 cells, indicating that activated calpains target key components of epithelial architecture during the course of CVB infection. Although a recent study has implicated a role for calpains in echovirus replication (Upla *et al.*, 2008), we found no evidence that calpains were specifically involved in CVB replication in Caco-2 cells as evidenced by our finding that calpain inhibitors and calpain

depletion with siRNAs did not decrease titers of newly replicated virus. Although we have previously shown that calpain 2 regulates CVB trafficking in polarized endothelial cells (Bozym *et al.*, 2010), we did not observe any effects of calpain inhibition on CVB entry into Caco-2 cells, suggesting that the role of calpains in facilitating CVB infection may differ between polarized cells types.

Polarized epithelial cells regulate the flow of ions and macromolecules across the epithelium by the presence of junctional complexes located at their apicolateral poles (Schneeberger and Lynch, 2004). We found that CVB infection induced a loss of junctonal integrity (as assessed by decrease in TER) within 4 h p.i. and that this change required calpain activity. We also found that CVB infection led to the relocalization of ZO-1, occludin, and several other junction-associated components such as β-catenin and E-cadherin (unpublished data). In addition, we found that occludin undergoes cleavage in CVB-infected cells and that both β-catenin and E-cadherin expression levels are diminished by CVB infection. These events require calpain activity as they were all blocked by a pharmacological inhibitor of calpains. Cleavage of occludin by calpains is also important in leukocyte transmigration across polarized airway epithelium (Chun and Prince, 2009), and calpains target both β-catenin (Benetti *et al.*, 2005) and E-cadherin (Rios-Doria *et al.*, 2003; Chun and Prince, 2009).

The relocalization of calpains from the cytoplasm to intracellular membranes has been speculated to play an important role in their activation (Leloup *et al.*, 2010). Consistent with this finding, attachment of a farnesyl anchor to calpain-2 triggers the strong induction of calpain activity (Leloup *et al.*, 2010). We found that calpain-2 relocalized from the cytoplasm to both the junctional complex and to internalized occludin-containing vesicles within 3 h following CVB infection. Interestingly, this time point corresponded with a significant decrease in $[Ca^{2+}]_i$ levels in CVB-infected cells and the loss of an inhibition of necrosis by small molecule inhibitors of calpains and those that disrupt $[Ca^{2+}]_i$ signaling. Taken together, these data suggest that calpains are activated within 2–3 h p.i. in CVB-infected cells that likely initiate a cascade of events, including cleavage of cell–cell contacts and junctional components, that ultimately leads to loss of membrane integrity and virus escape.

The mechanism of cell death we observed in several polarized intestinal epithelial cell lines differs markedly from the apoptotic cell death induced by CVB in nonpolarized cells [such as HeLa cells (Carthy *et al.*, 1998, 2003; Yuan *et al.*, 2003), pancreatic β-cells (Rasilainen *et al.*, 2004), and neurons (Joo *et al.*, 2002; Feuer *et al.*, 2003)]. The reasons for the induction of divergent cell death pathways between polarized and nonpolarized cells are likely complex and may be due to inherent differences in $Ca2^+$ regulation and/or signaling (such as in differences in the expression and cellular localization of IP3Rs; Colosetti *et al.*, 2003) in the expression, localization, and/or activation of innate immune-associated components (Hershberg, 2002; Cario *et al.*, 2007) or in the expression of signaling molecules that are associated with the regulation of cell death. Another possibility is that the composition and/or regulation of paracellular junctions of polarized epithelia play key roles in the regulation of cell death pathways in response to microbial assault. For example, as enterocytes display high rates of turnover, they have developed highly regulated means of cell death regulation, which have been linked to the integrity of their cell–cell contacts and most notably to the presence of E-cadherin. For example, loss of E-cadherin localization at epithelial junctions induces anoikis (Fouquet *et al.*, 2004; Lugo-Martinez *et al.*, 2009), a form of apoptosis induced by loss of cell–matrix interactions. Interestingly, the expression of a calpain-mediated cleavage fragment of E-cadherin potentiates cell death in epithelial cells (Rios-Doria and Day, 2005), and cleavage of the β-catenin binding domain of E-cadherin is associated with the induction of apoptosis (Vallorosi *et al.*, 2000). We observed that cleavage of occludin and decreases in E-cadherin and β-catenin expression occurred in a calpain-dependent manner in CVB-infected Caco-2 cells. Although we do not know whether these events are responsible for the induction of necrosis in CVB-infected polarized epithelia or are merely nonspecific events associated with calpain activation, it is attractive to speculate that the divergent mechanism of cell death observed in polarized versus nonpolarized epithelial cells may be the result of calpain-mediated cleavage of junction-associated components that serve to induce alternative mechanisms of cell death.

The results of our study indicate that cell death in CVB-infected Caco-2 cells occurs by a caspase-independent mechanism that instead depends on the activity of PLC, subsequent release of $[Ca^{2+}]_i$ from IP_3Rs, and the activation of calpains. These findings illustrate the unique mechanisms by which enteroviruses, and perhaps other viral pathogens, coopt intracellular signaling pathways in polarized cell monolayers to promote their entry, replication, and eventual spread.

MATERIALS AND METHODS

Cell culture and viruses

Caco-2 (ATCC) and HeLa (CCL-2) cells were cultured in modified Eagle's medium (MEM) supplemented with 10% fetal bovine serum, nonessential amino acids, sodium pyruvate, and penicillin/streptomycin. Caco-2 (BBE clone) cells were grown in DMEM-H supplemented with 10% fetal bovine serum and penicillin/streptomycin. CVB3-RD was expanded and purified as described previously (Coyne and Bergelson, 2006). Unless otherwise stated, all infections were performed with a multiplicity of infection (MOI) of 1–5 particle-forming units (PFU)/cell.

Antibodies

Mouse anti–enterovirus VP1 (Ncl-Entero) was obtained from Novocastra Laboratories (Newcastle upon Tyne, UK). Alexa Fluor–conjugated secondary antibodies, PI, phalloidin, mouse or rabbit anti–ZO-1, -occludin, or -β-catenin, and Annexin V were purchased from Invitrogen (Carlsbad, CA). Rabbit anti–caspase-3 and E-cadherin antibodies were purchased from Cell Signaling (Danvers, MA). Mouse anti-paxillin antibody was purchased from Abcam (Cambridge, MA); mouse anti-talin and mouse anti-vinculin antibodies were purchased from Sigma (St. Louis, MO); and goat anti–calpain -1 and -2 antibodies were purchased from Santa Cruz Biotechnology (Santa Cruz, CA).

Pharmacological inhibitors

CSA (5 μM), Z-Val-Phe-CHO (5 μM), and Z-VAD-FMK (20 μM) were purchased from Calbiochem (Gibbstown, NJ); U73122 (1 μM), Bapta-AM (10 μM), 2-APB (30 μM), caffeine (1 mM), CPA (10 μM), ruthenium red (5 μM), and thapsigargin (3 μM) were purchased from Sigma.

TER measurements

TER measurements were performed using an ohmmeter (EVOM; World Precision Instruments, Sarasota, FL) on cells grown on Transwell-collagen (COL) inserts for a minimum of 3 d. When cells exhibited R_T values of at least 600 Ω-cm^2, monolayers were infected with CVB (5–10 PFU/cell) at 37°C. At the indicated times, cells were removed and TER measured. All measurements were background corrected using a blank insert without cells.

Immunofluorescence microscopy

Caco-2 monolayers grown in collagen-coated chamber slides (BD Biosciences, San Jose, CA) were exposed to CVB at the indicated MOIs for 8 h (or the indicated time) at 37°C. The cells were then washed and fixed with ice-cold methanol or paraformaldehyde and permeabilized with Triton X-100. Monolayers were incubated with primary antibody, washed, and incubated with Alexa Fluor–488– or -594–conjugated secondary antibodies, washed, and then mounted with Vectashield containing 4′,6-diamidino-2-phenylindole (DAPI). PI and Annexin V staining was performed following the manufacturer's protocol. Briefly, cells were washed with phosphate-buffered saline (PBS), Annexin V-488 conjugate, and/or PI were added in annexin binding buffer (10 mM HEPES, 140 mM NaCl, 2.5 mM $CaCl_2$, pH 7.4) for 15 min at room temperature. Cells were rinsed in annexin binding buffer and then fixed with methanol and mounted with Vectashield containing DAPI. Images were captured with an Olympus IX81 inverted microscope equipped with a motorized stage or with an Olympus (Tokyo, Japan) Fluoview 1000 laser scanning microscope. Images of infected cells (PI and Annexin V) were taken using an Olympus Pan Apo 10×/0.28 NA dry objective, whereas all other images were taken with an Olympus PlanApo 60×/1.42 NA oil objective. Quantification of percent positive cells was performed using ImageJ (National Institutes of Health) analysis, where a minimum of three fields per condition were counted (at least 600 cells total). Cells were counted via DAPI staining, and positive cells were counted in the appropriate channel for the condition.

Ratiometric calcium imaging

Cells grown on collagen-coated, glass-bottom, 35-mm dishes (MatTek, Ashland, MA) were loaded with Fura-2 AM (1 μM; Invitrogen) for 30 min at 37°C. Cells were rinsed three times and bathed in a final volume of 1 ml of Ca^{2+}- and Mg^{2+}-free PBS. Images were captured on an Olympus IX81 motorized inverted microscope equipped with a Hamamatsu (Shizuoka, Japan) Orca-R2 CCD camera, a Sutter Lambda (Novato, CA) 10-3 High Speed filter wheel system, and an Olympus UApo/340 20× objective with an NA of 0.75 . Images were acquired using Slidebook 5.0 advanced imaging software. Selected cells were chosen [60 regions of interest (ROI)/dish], and images were captured at both excitation 340 and 380 nm every 10 s for 10 min (experiments were performed a minimum of three times). Thapsigargin was added to dishes after baseline was established (t = 50 s). Intensity ratios for selected ROIs were calculated using Slidebook 5.0, and representative traces for each experiment were plotted as a function of time (Figures 6A and 7, A and C). Images were pseudocolored (using Slidebook 5.0) to better visualize $[Ca^{2+}]_i$ mobilization with blue (low Ca_i^{2+}) and red (high Ca_i^{2+}). Overall changes in fluorescence intensity ratio (340/380) were calculated by subtracting the resting intensity ratio from the maximum intensity ratio achieved after thapsigargin addition.

Live cell calcium imaging

Caco-2 cells were grown to confluence on collagen-coated, glass-bottom, 35-mm dishes as stated earlier in the text. For virus experiments, CVB was added to the dish at MOI = 5 and placed at 37°C for 1.5 h. At this time, Fura-2 AM was added to the dish, and infection was allowed to continue for 30 min at 37°C. Medium was then removed, and cells were washed three times and placed in a final volume of 1 ml of Ca^{2+}/Mg^{2+}-free PBS. Dishes were placed on a 37°C temperature-controlled stage insert (Bioptechs, Butler, PA) mounted over an Olympus IX81 microscope (described in detail earlier in the text). Images were captured (from ~60 ROIs per experiment) at both 340 and 380 nm every 10 min for 1 h. Intensity ratios were calculated using Slidebook 5.0, with representative traces plotted as a function of time (Figure 6C). For uninfected control experiments, cells were incubated for 1.5 h in the absence of CVB, incubated with Fura-2AM for 30 min at 37°C, rinsed, and imaged as described earlier in the text.

siRNA transfections

siRNAs against calpain-1 (5′-GGCAGCUUUCGCUUGUUCCtt-3′) and calpain-2 (5′-GGCAGCUUUCGCUUGUUCCtt-3′) were synthesized by Integrated DNA Technologies (Newark, NJ). siRNAs to IP_3R-1 and -3 have been described (Bozym *et al.*, 2010). Cells were transfected using HiPerfect (Qiagen, Chatsworth, CA), according to the manufacturer's protocol or were delivered by nucleofection with an Amaxa nucleofection device (solution T, program B-24).

Statistical analysis

Data are presented as mean ± SD. One-way analysis of variance and Bonferroni's correction for multiple comparisons were used to determine statistical significance ($p < 0.05$ or < 0.001).

ACKNOWLEDGMENTS

We are grateful to Kevin Foskett for helpful advice and suggestions. This work was supported by funding from the National Institutes of Health (R01AI081759 to C.B.C. and R01AI52281 to J.M.B.).

REFERENCES

Agol VI, Belov GA, Bienz K, Egger D, Kolesnikova MS, Raikhlin NT, Romanova LI, Smirnova EA, Tolskaya EA (1998). Two types of death of poliovirus-infected cells: caspase involvement in the apoptosis but not cytopathic effect. Virology 252, 343–353.

Barco A, Feduchi E, Carrasco L (2000). Poliovirus protease 3C(pro) kills cells by apoptosis. Virology 266, 352–360.

Benetti R, Copetti T, Dell'Orso S, Melloni E, Brancolini C, Monte M, Schneider C (2005). The calpain system is involved in the constitutive regulation of beta-catenin signaling functions. J Biol Chem 280, 22070–22080.

Bozym RA, Morosky SA, Kim KS, Cherry S, Coyne CB (2010). Release of intracellular calcium stores facilitates coxsackievirus entry into polarized endothelial cells. PLoS Pathog 6.

Cardenas C *et al.* (2010). Essential regulation of cell bioenergetics by constitutive InsP3 receptor Ca2+ transfer to mitochondria. Cell 142, 270–283.

Cario E, Gerken G, Podolsky DK (2007). Toll-like receptor 2 controls mucosal inflammation by regulating epithelial barrier function. Gastroenterology 132, 1359–1374.

Carthy CM, Granville DJ, Watson KA, Anderson DR, Wilson JE, Yang D, Hunt DW, McManus BM (1998). Caspase activation and specific cleavage of substrates after coxsackievirus B3-induced cytopathic effect in HeLa cells. J Virol 72, 7669–7675.

Carthy CM *et al.* (2003). Bcl-2 and Bcl-xL overexpression inhibits cytochrome c release, activation of multiple caspases, and virus release following coxsackievirus B3 infection. Virology 313, 147–157.

Chandramohanadas R, Davis PH, Beiting DP, Harbut MB, Darling C, Velmourougane G, Lee MY, Greer PA, Roos DS, Greenbaum DC (2009). Apicomplexan parasites co-opt host calpains to facilitate their escape from infected cells. Science 324, 794–797.

Chun J, Prince A (2009). TLR2-induced calpain cleavage of epithelial junctional proteins facilitates leukocyte transmigration. Cell Host Microbe 5, 47–58.

Colosetti P, Tunwell RE, Cruttwell C, Arsanto JP, Mauger JP, Cassio D (2003). The type 3 inositol 1,4,5-trisphosphate receptor is concentrated at the tight junction level in polarized MDCK cells. J Cell Sci 116, 2791–2803.

Coyne CB, Bergelson JM (2006). Virus-induced Abl and Fyn kinase signals permit coxsackievirus entry through epithelial tight junctions. Cell 124, 119–131.

Festjens N, Vanden Berghe T, Vandenabeele P (2006). Necrosis, a well-orchestrated form of cell demise: signalling cascades, important mediators and concomitant immune response. Biochim Biophys Acta 1757, 1371–1387.

Feuer R, Mena I, Pagarigan RR, Harkins S, Hassett DE, Whitton JL (2003). Coxsackievirus B3 and the neonatal CNS: the roles of stem cells,

developing neurons, and apoptosis in infection, viral dissemination, and disease. Am J Pathol 163, 1379–1393.
Fouquet S, Lugo-Martinez VH, Faussat AM, Renaud F, Cardot P, Chambaz J, Pincon-Raymond M, Thenet S (2004). Early loss of E-cadherin from cell-cell contacts is involved in the onset of Anoikis in enterocytes. J Biol Chem 279, 43061–43069.
Franco SJ, Rodgers MA, Perrin BJ, Han J, Bennin DA, Critchley DR, Huttenlocher A (2004). Calpain-mediated proteolysis of talin regulates adhesion dynamics. Nat Cell Biol 6, 977–983.
Glading A, Uberall F, Keyse SM, Lauffenburger DA, Wells A (2001). Membrane proximal ERK signaling is required for M-calpain activation downstream of epidermal growth factor receptor signaling. J Biol Chem 276, 23341–23348.
Hershberg RM (2002). The epithelial cell cytoskeleton and intracellular traffickingVPolarized compartmentalization of antigen processing and Toll-like receptor signaling in intestinal epithelial cells. Am J Physiol Gastrointest Liver Physiol 283, G833–G839.
Hoyer-Hansen M *et al.* (2007). Control of macroautophagy by calcium, calmodulin-dependent kinase kinase-beta, and Bcl-2. Mol Cell 25, 193–205.
Hoyer-Hansen M, Jaattela M (2007). Connecting endoplasmic reticulum stress to autophagy by unfolded protein response and calcium. Cell Death Differ 14, 1576–1582.
Jayaraman T, Marks AR (1997). T cells deficient in inositol 1,4,5-trisphosphate receptor are resistant to apoptosis. Mol Cell Biol 17, 3005–3012.
Joo CH, Kim YK, Lee H, Hong H, Yoon SY, Kim D (2002). Coxsackievirus B4-induced neuronal apoptosis in rat cortical cultures. Neurosci Lett 326, 175–178.
Lebart MC, Benyamin Y (2006). Calpain involvement in the remodeling of cytoskeletal anchorage complexes. FEBS J 273, 3415–3426.
Lee JM, Zipfel GJ, Choi DW (1999). The changing landscape of ischaemic brain injury mechanisms. Nature 399, A7–A14.
Leloup L, Shao H, Bae YH, Deasy B, Stolz D, Roy P, Wells A (2010). m-Calpain activation is regulated by its membrane localization and by its binding to phosphatidylinositol 4,5-bisphosphate. J Biol Chem 285, 33549–33566.
Liu X, Van Vleet T, Schnellmann RG (2004). The role of calpain in oncotic cell death. Annu Rev Pharmacol Toxicol 44, 349–370.
Lopez-Guerrero JA, Alonso M, Martin-Belmonte F, Carrasco L (2000). Poliovirus induces apoptosis in the human U937 promonocytic cell line. Virology 272, 250–256.
Lugo-Martinez VH, Petit CS, Fouquet S, Le Beyec J, Chambaz J, Pincon-Raymond M, Cardot P, Thenet S (2009). Epidermal growth factor receptor is involved in enterocyte anoikis through the dismantling of E-cadherin-mediated junctions. Am J Physiol Gastrointest Liver Physiol 296, G235–G244.
Mattson MP (2000). Apoptosis in neurodegenerative disorders. Nat Rev Mol Cell Biol 1, 120–129.
Michetti M, Salamino F, Tedesco I, Averna M, Minafra R, Melloni E, Pontremoli S (1996). Autolysis of human erythrocyte calpain produces two active enzyme forms with different cell localization. FEBS Lett 392, 11–15.
Morens DM, Pallansch M (1995). Human Enterovirus Infections, Washington, DC: American Society for Microbiology.
Orrenius S, Zhivotovsky B, Nicotera P (2003). Regulation of cell death: the calcium-apoptosis link. Nat Rev Mol Cell Biol 4, 552–565.
Rami A (2003). Ischemic neuronal death in the rat hippocampus: the calpain-calpastatin-caspase hypothesis. Neurobiol Dis 13, 75–88.
Rasilainen S, Ylipaasto P, Roivainen M, Lapatto R, Hovi T, Otonkoski T (2004). Mechanisms of coxsackievirus B5 mediated beta-cell death depend on the multiplicity of infection. J Med Virol 72, 586–596.
Rios-Doria J, Day KC, Kuefer R, Rashid MG, Chinnaiyan AM, Rubin MA, Day ML (2003). The role of calpain in the proteolytic cleavage of E-cadherin in prostate and mammary epithelial cells. J Biol Chem 278, 1372–1379.
Rios-Doria J, Day ML (2005). Truncated E-cadherin potentiates cell death in prostate epithelial cells. Prostate 63, 259–268.
Sattler R, Tymianski M (2000). Molecular mechanisms of calcium-dependent excitotoxicity. J Mol Med 78, 3–13.
Schneeberger EE, Lynch RD (2004). The tight junction: a multifunctional complex. Am J Physiol Cell Physiol 286, C1213–C1228.
Sugawara H, Kurosaki M, Takata M, Kurosaki T (1997). Genetic evidence for involvement of type 1, type 2 and type 3 inositol 1,4,5-trisphosphate receptors in signal transduction through the B-cell antigen receptor. EMBO J 16, 3078–3088.
Trump BF, Berezesky IK (1996). The role of altered [Ca2+]i regulation in apoptosis, oncosis, and necrosis. Biochim Biophys Acta 1313, 173–178.
Upla P, Marjomaki V, Nissinen L, Nylund C, Waris M, Hyypia T, Heino J (2008). Calpain 1 and 2 are required for RNA replication of echovirus 1. J Virol 82, 1581–1590.
Vallorosi CJ, Day KC, Zhao X, Rashid MG, Rubin MA, Johnson KR, Wheelock MJ, Day ML (2000). Truncation of the beta-catenin binding domain of E-cadherin precedes epithelial apoptosis during prostate and mammary involution. J Biol Chem 275, 3328–3334.
van Kuppeveld FJ, Hoenderop JG, Smeets RL, Willems PH, Dijkman HB, Galama JM, Melchers WJ (1997). Coxsackievirus protein 2B modifies endoplasmic reticulum membrane and plasma membrane permeability and facilitates virus release. EMBO J 16, 3519–3532.
Wang KK (2000). Calpain and caspase: can you tell the difference? Trends Neurosci 23, 20–26.
Xu K, Tavernarakis N, Driscoll M (2001). Necrotic cell death in C. elegans requires the function of calreticulin and regulators of Ca(2+) release from the endoplasmic reticulum. Neuron 31, 957–971.
Yuan JP, Zhao W, Wang HT, Wu KY, Li T, Guo XK, Tong SQ (2003). Coxsackievirus B3-induced apoptosis and caspase-3. Cell Res 13, 203–209.
Zhou Y, Frey TK, Yang JJ (2009). Viral calciomics: interplays between Ca2+ and virus. Cell Calcium 46, 1–17.
Zong WX, Thompson CB (2006). Necrotic death as a cell fate. Genes Dev 20, 1–15.